

# Filipin and Its Interaction with Cholesterol in Aqueous Media Studied Using Static and Dynamic Light Scattering

MIGUEL A. R. B. CASTANHO,<sup>1,\*</sup> WYN BROWN,<sup>2</sup> and MANUEL J. E. PRIETO<sup>1</sup>

<sup>1</sup>Centro de Química Física Molecular, Complexo I, Instituto Superior Técnico, 1096 Lisboa Codex, Portugal; and

<sup>2</sup>Physical Chemistry Department, University of Uppsala, Box 532, 751 21 Uppsala, Sweden

## SYNOPSIS

Aggregation of filipin in aqueous medium and filipin-induced changes in cholesterol micelles have been studied using intensity and dynamic light scattering. The dependencies of filipin aggregate dimensions on concentration, solvent, and temperature were studied, and revealed that the aggregates do not have a well-defined geometry, i.e., a critical micelle concentration cannot be detected and stable structures are not formed. The aggregates are of size  $R_g \approx 110$  nm and  $R_h \approx 63$  nm, referring to the radius of gyration and hydrodynamic radius, respectively. In the concentration range studied ( $1 \mu M < C < 30 \mu M$ ), a low molecular weight species (monomer/dimer) is always present together with the aggregates. In ethanol/water mixtures, large ( $R_g \approx 500$  nm), narrow distribution aggregates are formed in the water volume fraction range  $0.45 < \Phi_{H_2O} < 0.65$ . Aggregation also occurs on changing the temperature; in the range 7–37°C, smaller aggregates (10–30 nm) form and the process is only partially reversible.

No pronounced effect of filipin on the structure of the cholesterol micelles was observed (a small increase in  $R_g$  and  $R_h$  is noted). These results rule out any "specificity" for the filipin interactions with cholesterol, which has been considered a key event in the filipin biochemical mode of action. A reevaluation of this question is suggested and some alternatives are advanced. © 1994 John Wiley & Sons, Inc.

## INTRODUCTION

Polyene macrolide antibiotics form a class of molecules having antifungal activity. Although they are able to provoke lysis in fungi, they are not effective against bacteria. Lampen et al.<sup>1</sup> explained this observation and showed that the key process for the toxicity of these antibiotics is their interaction with plasma membrane sterols, which are almost non-existent in bacterial membranes.

The aggregation of polyene antibiotics and sterols in a 1 : 1 stoichiometry, forming pores through the membrane or through the membrane layers, is a widely accepted model for the interaction of some polyene antibiotics (such as amphotericin B and nystatin) with sterols (for a review see Ref. 2 and references therein). But for other antibiotics (such

as filipin—Figure 1) their mode of action remains unknown, despite numerous investigations. Three models have been proposed for filipin-induced aggregation. These postulate highly specific interactions between filipin and sterol molecules. Two of the models are based on the formation of 1 : 1 aggregates, but with different dimensions and locations (a large planar aggregate inside the hydrophobic core of the membrane in one case<sup>3</sup> and a small aggregate with 8 molecules in the aqueous medium, at the membrane surface, in the other case<sup>4</sup>). The third model considers the formation of mixed aggregates of unspecified size and structure in the upper leaflet of the membrane.<sup>5</sup> However, the only approach yet used to study the structure of eventual mixed aggregates<sup>6</sup> was recently shown to be incorrect.<sup>7</sup> Subsequently, a new biochemical mode of action was proposed for filipin, independent of the presence of sterols.<sup>8</sup> Incorporation of filipin in sterol-free model membranes was demonstrated (a partition coeffi-

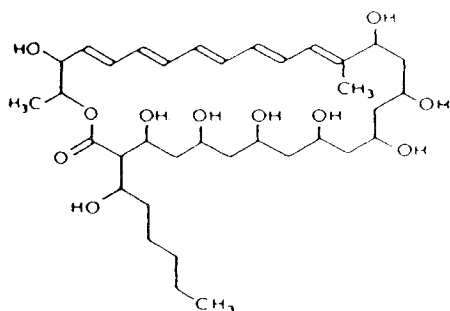


Figure 1. Molecular structure of filipin III.

cient of  $K_p = 3.4 \times 10^3$  was obtained; see Ref. 9). Thus, the nature of the interaction between filipin and cholesterol remains an open question.

A systematic study is now being carried out to elucidate this question. In a previous work, the ability of cholesterol to induce exciton interaction between the polyenic chromophores of filipin and of nystatin was demonstrated and studied using fluorescence and absorption spectroscopy.<sup>7</sup> In another study, the self-association of cholesterol into rod-like micelles in aqueous medium was examined using light scattering techniques.<sup>10</sup> We are currently using static and dynamic light scattering to elucidate (a) the structure of filipin aggregates in an aqueous medium; and (b) the changes in the cholesterol micelles and filipin aggregates, in the presence of each other. These are key questions concerning our understanding of polyene antibiotics and their mode of action.

Amphotericin B and nystatin, other polyene macrolide antibiotics, interact differentially with sterols depending on their state of aggregation.<sup>11-13</sup> The self-association of polyene macrolide antibiotics in aqueous media is due to their amphipatic nature. As can be seen from the structure of filipin (Figure 1), the hydrophobic part of the macrolide ring is determined by the double-bonded system, while the hydrophilic part is determined by the series of hydroxyl groups.

Most of the studies so far carried out on polyene self-association in aqueous media have used amphotericin B or a mixture: amphotericin B/deoxycholate, known commercially as "Fungizone." Rinert et al.<sup>14</sup> used CD, absorption spectroscopy, and static light scattering techniques to study "fungizone," and concluded that aggregates of  $2 \times 10^6$  daltons are formed, representing relatively labile aggregates of  $2 \times 10^3$  molecules. The existence of two or more antibiotic-aggregated forms in alcoholic solutions, as a function of the ethanol concentration, was proposed to account for the complex behavior

detected with CD spectroscopy. With static light scattering, the formation of an aggregate with decreasing molar mass is detected on changing from 30 to 50% ethanol in the medium.

Ernst et al.<sup>15</sup> proposed that the close packing of a few molecules could occur inside larger aggregates, which Hemenger et al.<sup>16</sup> proposed as being "linear polymers." The formation of dimers for a series of heptaene antibiotics was proposed by Mazerski et al.<sup>17</sup> According to these authors, the "nonsoluble" polyenes form oligomers that self-associate into aggregates.

For filipin, the formation of large (radius approximately 50 nm), and loose aggregates, in which all the molecules are accessible to the solvent, has been reported.<sup>9</sup> This conclusion was based on fluorescence quenching and anisotropy results and on a fit to a modified turbidity spectrum of the aggregate. A value for the critical micelle concentration (CMC) was also reported as 1–2  $\mu M$ .<sup>7,9</sup> In this study, these questions are revisited with a different approach.

Norman et al.<sup>6</sup> used studies carried out in aqueous solution and deduced that filipin forms specific complexes with sterols. However, this conclusion was refuted<sup>7</sup> and a filipin self-interaction induced by cholesterol was demonstrated. This observation, together with the interaction of filipin with sterol-free membranes,<sup>8,9</sup> raises the question whether a filipin-sterol complex is formed.

## EXPERIMENTAL

### Materials and Preparation

Filipin was obtained from Sigma and used as received. This antibiotic is a mixture of four macrolides,<sup>18</sup> with minor differences in their structures, the major component being the fraction known as filipin III (Figure 1). The concentration of filipin was determined by uv-visible absorption spectroscopy, using the molar extinction coefficients previously reported.<sup>9</sup> Filipin stock solutions in Tris HCl (BDH, London) buffer (50 mM, pH 7.4, NaCl 10 mM; 2% v/v in ethanol) or in spectroscopic-grade ethanol (Kemetyl, Stockholm) were kept in the dark, at 4°C. Dilution of filipin stock solutions were made with buffer or with a cholesterol solution in buffer was used to prepare the samples in aqueous solution. Water/ethanol solutions of filipin were prepared by dilution of the stock solution in ethanol with the appropriate volume of a mixture ethanol/buffer.

Neither filipin, nor cholesterol, have electrolytic

groups. In this way, a buffered solution would not be necessary. However, we decided to use it to be coherent with our previous studies and for the sake of the correlation between the data presented here and in previous and/or future studies.

Solutions of cholesterol micelles were prepared as previously reported.<sup>10</sup> All solutions were incubated in the dark for 15 min before being filtered with a Millex-HV Filter unit (0.45  $\mu\text{m}$ ). The solution preparation procedure gave solutions that were essentially dust free. This was shown by direct examination of the solutions in the scattering cells under laser illumination as well as the stability of the scattered signal and also by the linearity of the angular dependence of the reduced scattered intensity  $KC/R_\theta$  (see Figure 2a).

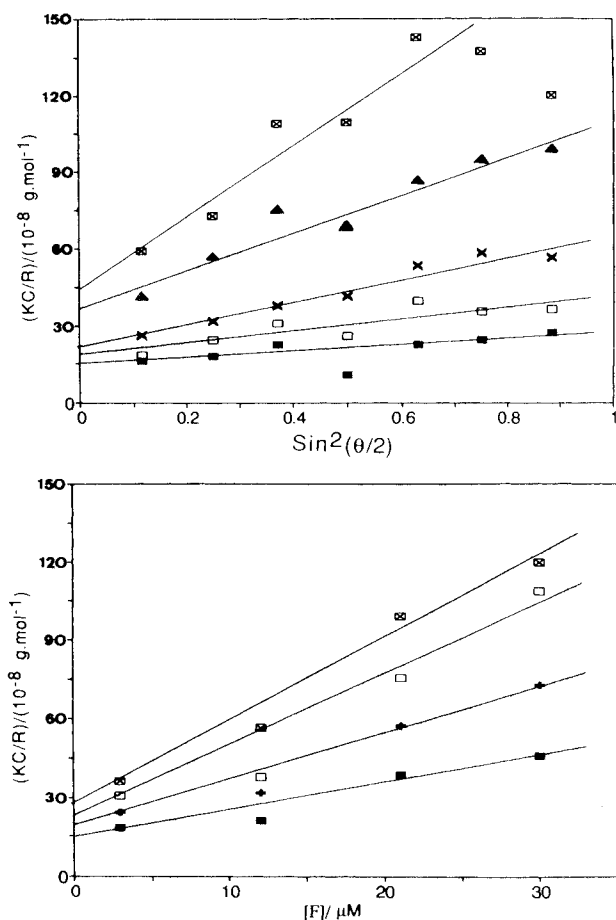


**Figure 2.** Angular (a) and concentration (b) dependencies of scattered light intensities relative to benzene. For the calculation of  $KC/R$ , an average value of  $dn/dC = 0.16 \text{ mL/g}$  was taken from the tables of Huglin.<sup>23</sup> The concentrations shown are  $\square$ , 30  $\mu\text{M}$ ;  $\blacktriangle$ , 21  $\mu\text{M}$ ;  $\times$ , 12  $\mu\text{M}$ ;  $\square$ , 3  $\mu\text{M}$ ; and  $\blacksquare$ , extrapolated values for 0  $\mu\text{M}$ . The angles shown are  $\square$ , 140°;  $\square$ , 75°;  $+$ , 60°; and  $\blacksquare$ , the extrapolated values for zero angle.

An incubation period of at least 2 h was maintained after filtration. As before,<sup>10</sup> the material used was washed with concentrated nitric acid, chloroform, and distilled water, and not subject to the action of any detergent.

Polarized dynamic light scattering ( $I_{VV}$ ) measurements were made using the apparatus and techniques described in the previous article and also in Ref. 19. The data were assembled using a wide-band multi- $\tau$  autocorrelator (ALV-3000) with 23 simultaneous sampling times, allowing characterization of relaxation time distributions extending over 8 decades. Average diffusion coefficients were estimated using the method of cumulants, with both second- and third-order terms. Inverse Laplace transformation (ILT) was made employing the algorithm REPES,<sup>20</sup> which is similar to Provencher's CONTIN<sup>21</sup> except that the former directly minimizes the sum of the squared differences between experimental and calculated intensity-intensity  $g_2(t)$  functions [ $g_2(t) = g_1^2(t)$ ] using nonlinear programming. For a system exhibiting a distribution of relaxation times, the field correlation function,  $g_1(t)$ , is described by the Laplace transform as a continuous function of the relaxation time  $\tau$ :

$$g_1(t) = \int_0^\infty A(\tau) e^{-t/\tau} d\tau$$

The range of relaxation times allowed in the fitting was usually between 0.5  $\mu\text{s}$  and 1 s with a density of 12 points per decade. Relaxation rates are obtained from the moments of the peaks in the relaxation time distribution or, if the peaks overlap, from the peak position. With a broad distribution of relaxation times, both inversion methods can yield multiple peaks in the "unsmoothed" analysis. The "smoothing" parameter ( $P$ ) was selected as 0.5 in all cases. This degree of smoothing corresponds to the default value of the so-called chosen solution in CONTIN. The influence of the smoothing parameter on the relaxation time distributions has been discussed by Nicolai et al.<sup>19</sup> Comparisons with simulated data are dealt with in the same article.

Mutual diffusion coefficients (calculated as  $D_m = \Gamma/\mathbf{q}^2$ ) and the relative amplitudes are obtained from the moments of the peaks and are given in the output of the program.  $\Gamma$  is the measured relaxation rate ( $\Gamma = \tau^{-1}$ ) and  $\mathbf{q}$  is the scattering vector.

Intensity light scattering measurements were performed with a photon-counting device supplied by Hamamatsu. The light source was a 3 mW He-Ne laser (632 nm). The reduced scattering intensity,

$C/I_r$ , was measured on the same solutions as used for the dynamic light scattering measurements, where the intensities are measured relative to benzene at each angle.

Apparent radii of gyration ( $R_g$ ) were estimated from the ratio of the slope to the intercept of plots of the angular dependence of the reduced scattering intensity ( $KC/R_\theta$ ) as shown for typical data in Figure 2a, where  $C$  is the concentration. The scattering constant is  $K = 4\pi^2 n_0^2 (dn/dC)^2 / (N_A \lambda^4)$ . The Rayleigh ratio used for benzene is  $8.51 \times 10^{-6} \text{ cm}^{-1}$ .<sup>22</sup> Since at the extremely low concentrations attainable for filipin in aqueous solution (maximum ca.  $30 \mu\text{M}$ ) it is not possible to measure  $dn/dC$  directly, an average value of  $dn/dC = 0.16 \text{ mL/g}$  for polysaccharides taken from the tables of Huglin<sup>23</sup> has been used in order to make an approximate estimation of the weight average molecular weight ( $M_w$ ) and the second virial coefficient  $A_2$ . The  $dn/dC$  has a small variation for a wide variety of polysaccharides.

Fluorescence measurements for evaluation of filipin exciton interaction were made as previously described.<sup>7</sup>

## RESULTS

### Filipin in Buffer

Intensity light scattering measurements were made on filipin dissolved in buffer (see experimental section). Plots of the reduced scattered intensity ( $KC/R_\theta$ ) were made as a function of  $\sin^2(\theta/2)$  as shown for typical data at different concentrations in Figure 2a. The scatter in the points is relatively high owing to the extremely low scattered intensity (about 50% of that for pure benzene at  $90^\circ$  used for calibration). For this reason each point has been measured five times and the data shown in the respective plots represent the average values. From the ratio of the slope to intercept of the  $C = 0$  line, the value of  $R_g = 110 \text{ nm}$  was estimated.

The data from plots such as those in Figure 2a are plotted vs concentration in Figure 2b for various angles. The line for zero angle was used to estimate the second virial coefficient:  $A_2 = 11.3 \times 10^{-3} \text{ mL/g}$ . The common intercept for the  $C = 0$  and  $\theta = 0$  lines in Figure 2a,b give  $M_w \approx 7 \times 10^6 \text{ g/mol}$ . It should be emphasized that these values are approximate due to the data scatter at the very low concentrations that are accessible to measurement.

Analysis of dynamic light scattering data by Laplace inversion to obtain the relaxation time distribution can prove illuminating and this approach has

been used widely in studies of polymer systems (see, for example, Ref. 19). Caution is necessary since the presence of noise on the correlograms may lead to spurious peaks. However, when the peaks are well separated and the overall trends in the data are systematic, such an approach can yield additional insights into complex systems in which several scattering components are present. This is the present situation. Although the scattering intensity is rather low, the data are reproducible and the results of the Laplace inversion (see, for example, Figure 3a) establish that the characteristic peaks are widely separated on the time scale and lead to systematic trends.

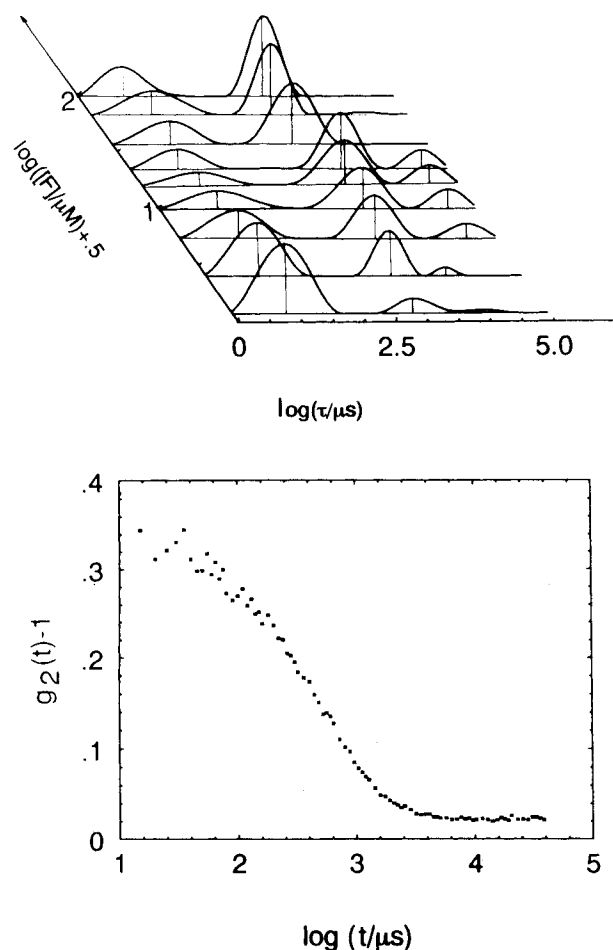


**Figure 3.** (a) Relaxation time distributions [ $\tau A(\tau)$  vs  $\log(\tau/\mu\text{s})$ ] from inverse Laplace transformation, for several filipin concentrations. The vertical axis (not shown) is  $\tau A(\tau)$  to provide an equal area representation, allowing direct comparison between different distributions. (b) Typical correlation function ( $\theta = 90^\circ$ ;  $25^\circ\text{C}$ ), obtained for a filipin concentration of  $30 \mu\text{M}$ , accumulated over 15 h.

**Table I. Parameters Characterizing Filipin Aggregates and Cholesterol Micelles in the Presence of Filipin<sup>a</sup>**

Compound	Solvent	Experimental Approach	Parameter	Value	Remarks
Filipin	Buffer	ILS	$R_g$ (nm)	110	
			$M \cdot 10^{-6}$ ( $g \cdot mol^{-1}$ )	7	
			$A_2 \cdot 10^3$ ( $cm^3 g^{-1}$ )	11.3	
		DLS	$R_{h,1}$ (nm)	1.5	b
			$R_{h,2}$ (nm)	63	b
			$R_{h,3}$ (nm)	2700	b
			$R_{h,7^\circ C}$ (nm)	1.5	
			$R_{h,17^\circ C}$ (nm)	1.5, 14	
			$R_{h,25^\circ C}$ (nm)	1.6, 32	
	Buffer/Ethanol	ILS	$R_{g,app}$ (nm)	585	$\Phi_{H_2O} = 0.45$
				505	$\Phi_{H_2O} = 0.55$
				440	$\Phi_{H_2O} = 0.65$
DLS	$R_{h,app}$ (nm)	333	$\Phi_{H_2O} = 0.65$		
		373	$\Phi_{H_2O} = .55; .45$		
		1.5	c		
Cholesterol	Buffer	ILS	$R_{g,app}$ (nm)	136–164	$[F]$ ( $\mu M$ ) = 0–29
		DLS	$R_{h,app}$ (nm)	63–68	$[F]$ ( $\mu M$ ) = 0–26

<sup>a</sup>  $\Phi_{H_2O}$ : volume fraction of water; DLS: dynamic light scattering; ILS: intensity light scattering. Unless otherwise stated, all values were obtained at 25°C.

<sup>b</sup> The relative weights of these components depend on the antibiotic concentration.

<sup>c</sup> Monomer/dimer (not present for all the values of  $\Phi_{H_2O}$ ).

Relaxation time distributions  $\tau A(\tau)$  vs  $\log \tau$  obtained by ILT of the correlation curves (Experimental) are shown in Figure 3a for filipin in buffer at various concentrations. At the higher concentrations ( $C > 7 \mu M$ ), the distributions are two peaked, while at  $C < 7 \mu M$  an additional very slow component is apparent. The peak of shortest relaxation time corresponds to the filipin monomer/dimer having a hydrodynamic radius of about 1.5 nm calculated using the Stokes–Einstein relationship from the diffusion coefficient at infinite dilution. The intermediate-sized aggregates have  $R_h \approx 63$  nm and the largest species  $R_h \approx 2700$  nm (Table I).

Figure 3b shows a typical correlation function for the solution having  $C = 30 \mu M$  filipin. These data were accumulated over 15 h at an average scattered intensity of 0.4 kHz (angle = 90°; 25°C).

The collected data for the apparent hydrodynamic radius  $(R_h)_{app}$  are displayed in Figure 4 in a logarithmic plot (see also Table I). There is no significant concentration dependence.

### Filipin/Ethanol Solutions

**Static Light Scattering.** The scattered intensity passes through a sharp maximum in the range

$\Phi_{H_2O}$  (fraction volume of water) = 0.40–0.75 as the solvent composition is changed as is shown in Figure 5 for the intensity ratio vs volume fraction water. The intensity has again fallen to a level approxi-

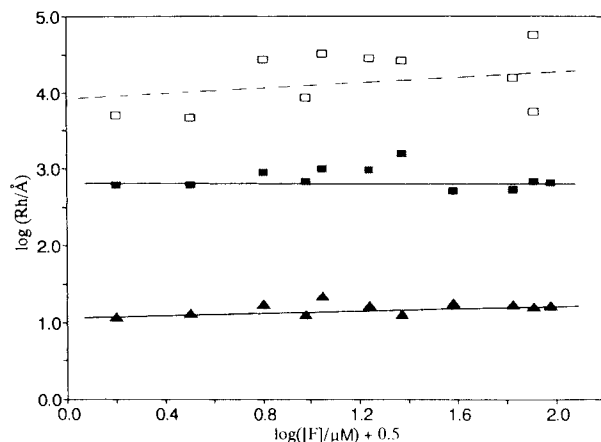


**Figure 4.** Hydrodynamic radii calculated from the data in Figure 3a, using the Stokes–Einstein relationship. The fastest component has  $R_h \approx 1.5$  nm, and can be ascribed to a filipin monomer/dimer. The second component has  $R_h \approx 63$  nm. The slowest component corresponds to  $R_h \approx 2700$  nm.

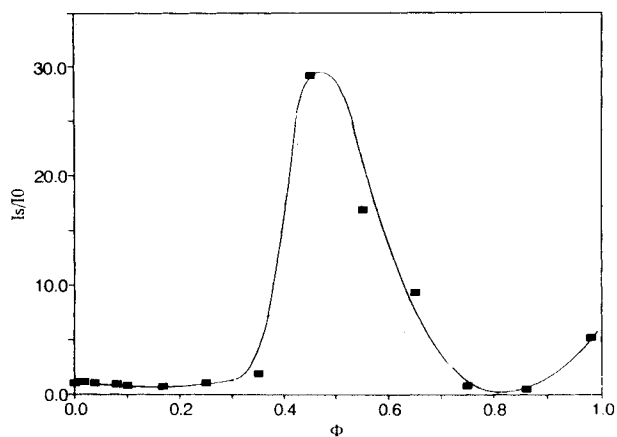


**Figure 5.** Absolute scattered intensities for filipin ( $20 \mu\text{M}$ ) in buffer/ethanol mixtures, normalized for the volume fraction of water of  $\Phi_{\text{H}_2\text{O}} = 0$ . The scattered intensity passes through a sharp maximum in the range  $0.40 < \Phi_{\text{H}_2\text{O}} < 0.75$ . A critical dependence for the filipin aggregates on solvent composition is also evident in Figures 7 and 8.

mately equal to that for the monomer/dimer above  $\Phi_{\text{H}_2\text{O}} = 0.75$ .

The angular dependence of the reduced intensity ( $C/I_r$ ) was determined for three compositions close to the maximum (Figure 6). The values ( $R_g$ )<sub>app</sub> = 440 nm ( $\Phi_{\text{H}_2\text{O}} = 0.65$ ), 505 nm ( $\Phi_{\text{H}_2\text{O}} = 0.55$ ), and 585 nm ( $\Phi_{\text{H}_2\text{O}} = 0.45$ ) were found, demonstrating a pronounced aggregation effect.

**Dynamic Light Scattering.** A typical correlation function is shown for the mixture with  $\Phi_{\text{H}_2\text{O}} = 0.45$

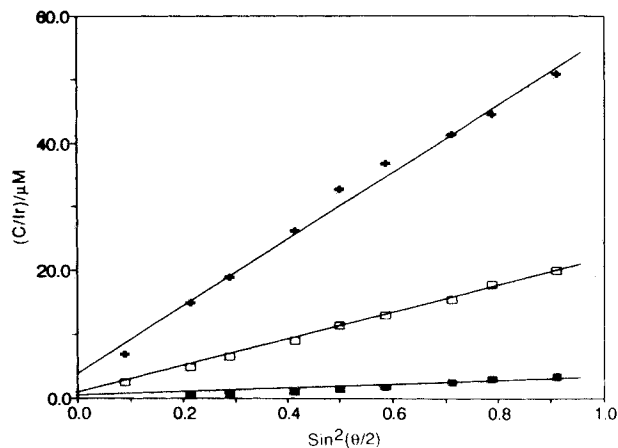


**Figure 6.** Reduced scattered intensity (relative to benzene)  $C/I_r$ , measured on the same samples as Figure 5, corresponding to  $\Phi_{\text{H}_2\text{O}} = 0.45$  (■),  $\Phi_{\text{H}_2\text{O}} = 0.55$  (□), and  $\Phi_{\text{H}_2\text{O}} = 0.65$  (+). Apparent radii of gyration were estimated from the ratio of the slope to intercept of the depicted plots.

water in Figure 7a. Relaxation time distributions are shown in Figure 7b obtained by ILT analysis of the correlation functions. In the lower part of the diagram covering the water volume fraction range up to  $\Phi_{\text{H}_2\text{O}} = 0.25$ , the monomer/dimer form of filipin is dominant in intensity with an increasing

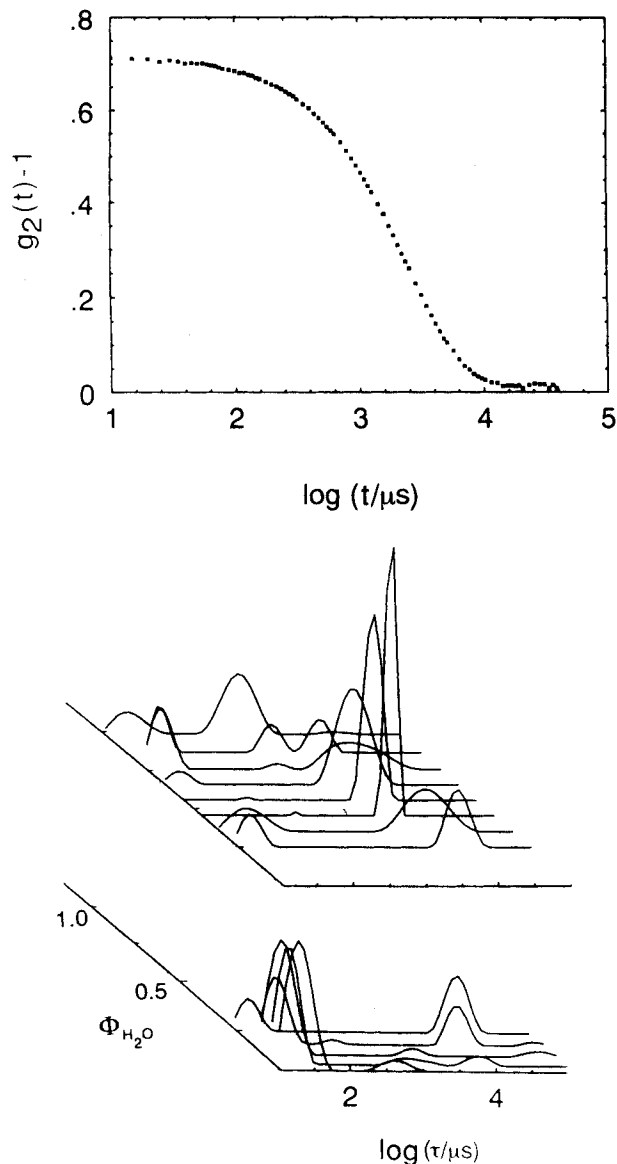


**Figure 7.** Dynamic light scattering analysis over the range  $0 < \Phi_{\text{H}_2\text{O}} < 0.98$ . A correlation curve (corresponding to  $\Phi_{\text{H}_2\text{O}} = 0.45$ ) is shown (a). The relaxation time distribution obtained by ILT analysis of the correlation curves are shown in (b). For the sake of simplicity, the ranges  $0 < \Phi_{\text{H}_2\text{O}} < 0.25$  (lower) and  $0.25 < \Phi_{\text{H}_2\text{O}} < 0.98$  (upper) in part (b) were separated (the distribution corresponding to  $\Phi_{\text{H}_2\text{O}} = 0.25$  is depicted in both levels for ease of comparison). The vertical axis (not shown) is  $\tau A(\tau)$  to provide equal area representation.

amplitude of an aggregated component of long relaxation time. In the upper part of Figure 7b, covering compositions  $\Phi_{\text{H}_2\text{O}} = 0.25\text{--}0.98$ , the dominance of the large aggregates in the range  $\Phi_{\text{H}_2\text{O}} = 0.45\text{--}0.75$  is clearly shown, and corresponds to the intensity maximum of Figure 5.

In terms of the hydrodynamic radius,  $R_h \approx 1.5$  nm for the monomer/dimer (Figure 8), while the aggregates gave the following values: 333 nm ( $\Phi_{\text{H}_2\text{O}} = 0.65$ ) and 373 nm ( $\Phi_{\text{H}_2\text{O}} = 0.55$  and  $\Phi_{\text{H}_2\text{O}} = 0.45$ ; see Table I).

### Filipin/Cholesterol Interaction

**Static Light Scattering.** The intensity scattered by filipin/cholesterol mixtures is independent of the composition. Figure 9 shows that there is a smooth increase in the apparent radius of gyration with increasing filipin content. This trend is paralleled by a corresponding increase in the hydrodynamic radius (see below; Figure 9).

**Dynamic Light Scattering.** As demonstrated previously,<sup>10</sup> the correlation function for cholesterol is single exponential and the relaxation time distribution single peaked. This situation prevails over the entire concentration range examined in solutions containing up to 30  $\mu\text{M}$  filipin and 10  $\mu\text{M}$  cholesterol. Thus no major change to the conformation of the cholesterol micelle occurs on addition of filipin. Figure 10 depicts the hydrodynamic radius as a function of the concentration of filipin in a 10  $\mu\text{M}$  cholesterol

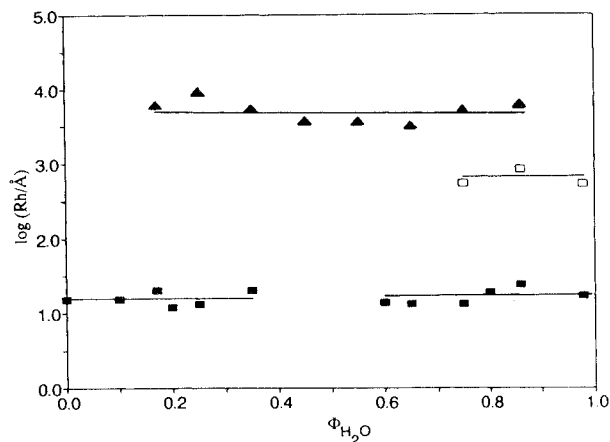


**Figure 8.** Hydrodynamic radii corresponding to the data in Figure 7b. The value for the monomer/dimer is  $R_h \approx 1.5$  nm. The peaks for  $\Phi_{\text{H}_2\text{O}} = 0.45$  and  $\Phi_{\text{H}_2\text{O}} = 0.55$  are narrow, reflecting low polydispersity (cf. Figure 7b). Typical aggregates for aqueous solutions appear only at  $\Phi_{\text{H}_2\text{O}} > 0.75$ .

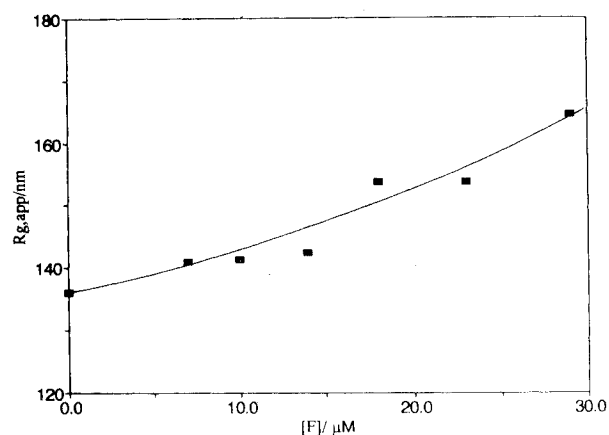


**Figure 9.** Apparent radii of gyration of cholesterol (10  $\mu\text{M}$ ) micelles in the presence of filipin. Apparent radii of gyration were calculated by the method indicated in the caption to Figure 6.

solution. There is a significant increase in  $R_h$  from a value of  $R_h = 63$  nm with 0% filipin to 68 nm with 26  $\mu\text{M}$  filipin both with a constant concentration of cholesterol (10  $\mu\text{M}$ ; see Table I).

### Influence of Temperature on Filipin Solutions in Buffer

**Dynamic Light Scattering.** Figure 11 shows relaxation time distributions for a filipin solution (concentration 21  $\mu\text{M}$ ) in buffer. At 7°C the monomer/dimer form of filipin is present but, with increasing temperature, an aggregate form appears that remains as the sole component at 37°C. The aggregation process is only partially reversible: lowering to temperature successively to 7°C leads to partial retention of the aggregate peak.

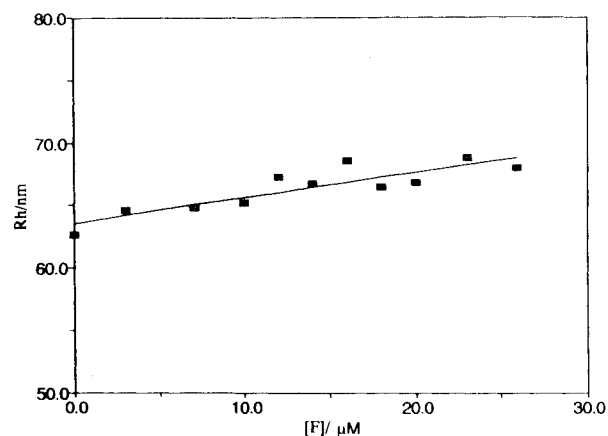


**Figure 10.** Hydrodynamic radii ( $R_h$ ) of the cholesterol (10  $\mu\text{M}$ ) micelles as a function of the filipin concentration.

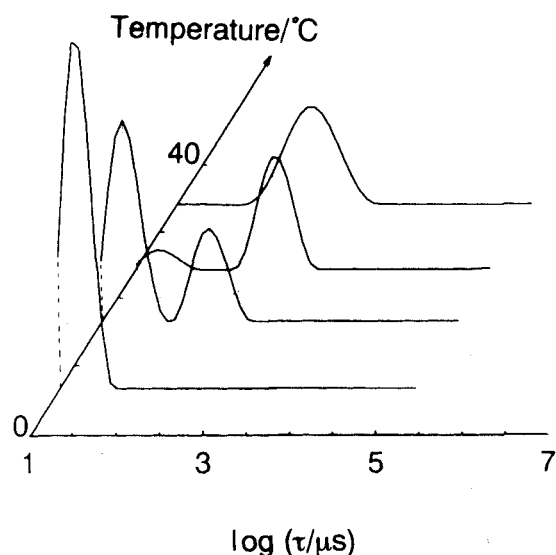


**Figure 11.** Relaxation time distributions for a filipin ( $21 \mu\text{M}$ ) solution in buffer as a function of temperature. Significant aggregation is seen as the temperature increases.

The apparent hydrodynamic radii of the aggregate peaks are summarized in Table I.

## DISCUSSION

Plots of the inverse particle scattering factor [ $P(\mathbf{q}, R)^{-1}$ ] vs  $\mathbf{q} \cdot R_g$  have been made for various models (sphere; coil and thin rod) using the relationships given by Schmitz.<sup>24</sup> These plots are shown in Figure 12. Data shown in Figure 2a at  $C = 0$  for filipin in buffer have been inserted and these suggest that an extended conformation is more likely than a spherical one. The data fall below the line for the rod, however, probably owing to excess scattering from dust/aggregates, and thus it is not possible to distinguish between the alternative models. We note that the value of  $R_g/R_h = 1.75$  is close to that for a randomly coiling structure. Burchard et al.<sup>25</sup> showed that the ratio  $R_g/R_h = 2.05$  results for polydisperse linear chains with excluded volume and 1.73 for random coils under ideal solvent conditions.

Depolarized scattering measurements were attempted, but these measurements proved prohibitive at the low scattering intensities of the solutions. The values of  $R_g$  (110 nm) and  $M_w$  ( $7 \times 10^6$ ) only indicate that the aggregates are large but of a form that cannot be clearly determined from the present data; for this reason most of the discussion is focused instead on changes found in the filipin aggregates under various conditions. Calculation of the equivalent

hard-sphere radius, using the relationship<sup>26</sup>  $R_{\text{eq}} = [3Mv_2/(4\pi N_A)]^{1/3}$  with the above values of  $R_g$  and  $M_w$ , and using the partial specific volume  $v_2 = 0.74 \text{ mL/g}$ , gives  $R_{\text{eq}} \approx 11 \text{ nm}$ , which provides a minimum dimension and emphasizes the aggregate extension.

The relaxation time distributions show that there is always an equilibrium with the monomer/dimer, with a substantial number density excess of the latter.

The present conclusions regarding the conformation of the filipin aggregates broadly concur with those made earlier,<sup>9</sup> i.e., that filipin forms aggregates of large dimensions in buffer at concentrations greater than approximately  $1 \mu\text{M}$ . Anisotropy and fluorescence quenching experiments showed the aggregates to be loose and open structures that is compatible with the labile structure suggested by the changes in the relaxation time distributions as a function of temperature. A similar structure has been proposed for amphotericin B in the fungizone preparation from the results of CD, uv-visible absorption, and static light scattering measurements. This involves a close packing of a few molecules<sup>15</sup> that assemble into a two molecule/unit cell helical polymer<sup>16</sup> that is relatively labile and has a mass of  $2 \times 10^6$  daltons and with  $R_g = 60 \text{ nm}$ .<sup>14</sup>

The results reported in this last reference on the aggregation state of amphotericin B in water/ethanol solutions are similar in some respects to

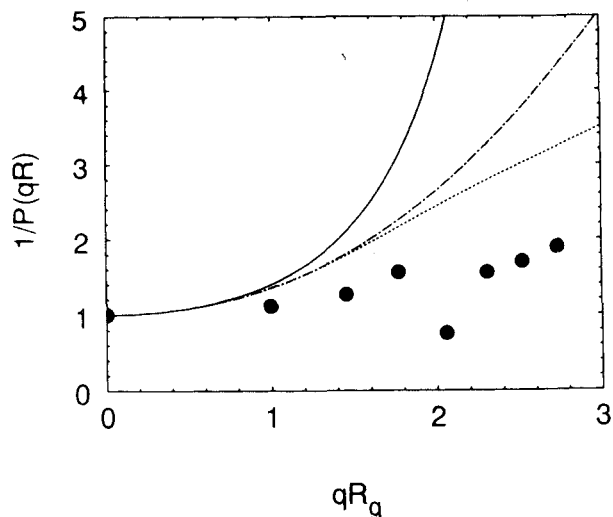


**Figure 12.** Inverse scattering factor for three model shapes (sphere, —; coil, - · - · - ·; thin rod, -----). The points are experimental data (zero concentration values from Figure 2a). The  $R_g$  value used for the experimental data was  $R_g = 110 \text{ nm}$ , deduced from Figure 2a (see text).

those found here for filipin, although there are important differences. Thus in both systems there exists a "critical" region at  $0.45 < \Phi_{\text{H}_2\text{O}} < 0.65$ , in which there is a pronounced tendency for aggregation, and the dimensions and distributions of the molecular species are critically determined by the solvent, demonstrating the role of solvent interactions on the structure of the aggregate. This narrow range of solvent composition is the only one where the monomer/dimer of filipin is not detected. One may speculate on the existence of intermolecular polyene chain interactions that could explain the detection of excitonic interaction between the chromophores of filipin.<sup>7</sup> Aggregated filipin in buffer forms excitons at concentrations near that regarded as its CMC (1  $\mu\text{M}$ ; Ref. 7). Considering the data in Figure 3a, the shortest relaxation time can be assigned to small aggregates with a size corresponding to the dimer (see following paragraph) and for which the orientations and proximities of the chromophores meet the restrictions needed for exciton interaction. As the concentration increases, the relative importance of these small aggregates decreases due to the formation of large labile aggregates, where these strict restrictions are not met.<sup>7</sup>

A radius of 0.55 nm can be calculated for the filipin molecule from volume considerations, evaluated by the method of Edward,<sup>27</sup> and a spherical shape. The stacking of two molecules with a solvation shell would correspond roughly to the measured value of  $R_h = 1.5$  nm.

The complex behavior detected for self-associated filipin as a function of temperature (Figure 11) provides other evidence for the labile structure of the aggregate. Critical temperatures are not detected in the range 7–40°C, but there is a pronounced tendency for aggregation as the temperature is raised: monomer/dimer is the sole species present at 7°C and only the aggregated form is detectable at 37°C. The same was observed by Richtering et al.<sup>28</sup> in a nonionic surfactant that forms percolation clusters with an open structure.

Taken together, the present results show that the aggregates of filipin are not micelles, i.e., there is no well-defined geometry nor a well-defined CMC and stable structures are not formed.

Archer<sup>29</sup> showed that, at 2°C the filipin sensitivity of *Mycoplasma mycoides* subspecies *capri* is independent of the membrane cholesterol content, in contrast to the results at 20°C. Furthermore, at 2°C sterol-free egg lecithin vesicles become very sensitive to filipin and the presence of cholesterol in the vesicles does not increase the sensitivity further. Considering the results of the present study, the different

results obtained by Archer at different temperatures may indicate a connection between the filipin aggregation state and its eventual interaction with membrane sterols.

Gruda and Dussault,<sup>11</sup> Tancrede et al.,<sup>12</sup> and Bolard et al.<sup>13</sup> proposed a correlation between the aggregation state of amphotericin B and its biochemical action. However, while the first indicates that ergosterol does not interact with monomeric amphotericin B (a similar conclusion was reached by Bolard et al.), the second group reported the opposite: monomeric antibiotics have an enhanced capacity to "bind" sterols. Both results were obtained using the same method,<sup>6</sup> which was shown to be incorrect because it does not probe sterol/antibiotic interactions but rather antibiotic/antibiotic exciton interactions.<sup>7</sup> Our results clearly show that no major alterations in the cholesterol micellar structure formed under the used conditions (proposed to be a long, thin, and stiff rod; Ref. 10) are induced in the presence of filipin, independent of the filipin concentration in the accessible range (and thus the aggregation state). This observation makes it clear that filipin and cholesterol do not interact in a highly specific manner in aqueous solution. Thus, the formation of antibiotic/sterol complexes in aqueous solution with a well-defined structure and stoichiometry is ruled out. The reported "specificity" of polyene antibiotics interaction with sterols, considered as the basic process of filipin's antibiotic action (see references in Ref. 7), needs reevaluation.

The increase in  $R_h$  and  $R_g$  of cholesterol micelles with increasing concentration of filipin (Figures 9 and 10) suggests aggregate growth. This may either mean adsorption of filipin at the cholesterol micellar surface (similar to that which occurs at the surface of cholesterol microcrystals; Ref. 7) or a stacking of filipin (linear) chains at the ends of the micelles. One may speculate that if the latter was the case, more pronounced variations in the detected parameters would be expected (namely, an increase in the ratio  $R_g/R_h$ ). The absence of exciton interaction in the systems studied precludes conclusions on this matter. However, it can be speculated that the many hydroxyl groups on the cholesterol micelle surface will cause a random clustering to particles of low mean segment density, similar to the association of nonionic micelles that was studied by Richtering et al.<sup>28</sup> According to the law of mass action, association should increase when the overall concentration is increased. This is the effect observed when filipin is added to cholesterol micelles, as well as the effect observed with the aggregation of filipin itself.

The conclusions reached in this study, together

with those of our previous studies and recently published works,<sup>8</sup> suggest a need to reevaluate the biochemical mode of action of filipin. Alternative models have been put forward. Krawczyk and Cukierman<sup>30</sup> proposed that filipin is involved in the formation of ion channels in lipid bilayers containing cholesterol, based on transmembrane conductance measurements. Milhaud<sup>8</sup> proposed permeability induction in the interfacial region at the boundaries of the filipin-phospholipid domains, independent of the presence of cholesterol. In biological systems, the action of filipin is more complex. The interaction of the polyene antibiotic filipin with membrane cholesterol inhibits membranous enzyme systems differentially<sup>31</sup> and lysis is not involved. Possibly filipin has only generalized actions at the membrane level, without a specific target.

This work has been supported by the Swedish Natural Science Research Foundation (NFR) and by Junta Nacional de Investigação Científica e Tecnológica (JNICT, Portugal). MARBC would also like to thank Junta Nacional de Investigação Científica e Tecnológica (JNICT) and the Swedish Institute for a grant and travel support in connection with his stay in Uppsala. We wish to thank Robert M. Johnsen for frequent discussions during the course of this work.

## REFERENCES

- Lampen, J. O., Arrow, P. M. & Safferman, R. S. (1960) *J. Bacteriol.* **80**, 200–206.
- Bolard, J. (1986) *Biochim. Biophys. Acta* **864**, 257–304.
- De Kruijff, B. & Demel, R. A. (1974) *Biochim. Biophys. Acta* **339**, 57–70.
- Elias, P. M., Friend, D. S. & Goerke, J. (1979) *J. Histochem. Cytochem.* **27**, 1247–1260.
- Severs, N. J. & Robenek, H. (1983) *Biochim. Biophys. Acta* **737**, 373–408.
- Norman, A. W., Demel, R. A., de Kruijff, B. & Van Deenen, L. L. M. (1972) *J. Biol. Chem.* **247**, 1918–1929.
- Castanho, M. A. R. B., Coutinho, A. & Prieto, M. J. E. (1992) *J. Biol. Chem.* **267**, 204–209.
- Milhaud, J. (1992) *Biochim. Biophys. Acta* **1105**, 307–318.
- Castanho, M. A. R. B. & Prieto, M. J. E. (1992) *Eur. J. Biochem.* **207**, 125–134.
- Castanho, M. A. R. B., Brown, W. & Prieto, M. J. E. (1992) *Biophys. J.* **63**, 1455–1461.
- Gruda, I. & Dussault, N. (1988) *Biochem. Cell Biol.* **66**, 177–183.
- Tancrede, P., Barwicz, J., Jutras, S. & Gruda, I. (1990) *Biochim. Biophys. Acta* **1030**, 289–295.
- Bolard, J., Legrand, J. P., Heitz, F. & Cybulska, B. (1991) *Biochemistry* **30**, 5707–5715.
- Rinnert, H., Thirion, C., Dupont, G. & Lematre, S. (1977) *Biopolymers* **16**, 2419–2427.
- Ernst, C., Grange, J., Rinnert, H., Dupont, G. & Lematre, J. (1981) *Biopolymers* **20**, 1575–1588.
- Hemenger, R. P., Kaplan, T. & Gray, L. J. (1983) *Biopolymers* **22**, 911–918.
- Mazerski, J., Bolard, J. & Borowski, E. (1982) *Biochim. Biophys. Acta* **719**, 11–17.
- Bergy, M. & Eble, T. (1968) *Biochemistry* **7**, 653–659.
- Nicolai, T., Brown, W. & Johnsen, R. M. (1990) *Macromolecules* **23**, 1165–1174.
- Jakes, J. (1988) *Czech. J. Phys. B* **38**, 1305–1316.
- Provencher, S. W. (1979) *Makromol. Chem.* **180**, 201–209.
- Pike, E. R., Pomeroy, W. R. M. & Vaughan, J. M. (1975) *J. Chem. Phys.* **62**, 3188–3192.
- Huglin, M. B. (1972) in *Light Scattering from Polymer Solutions*, Huglin, M. B., Ed. Academic Press, London, pp. 216–225.
- Schmitz, K. S. (1990) *An Introduction to Dynamic Light Scattering by Macromolecules*, Academic Press, New York, p. 22.
- Burchard, W., Schmidt, M. & Stockmayer, W. H. (1980) *Macromolecules* **13**, 1265–1272.
- Tanford, C. (1965) *Physical Chemistry of Macromolecules*, Wiley, New York, p. 356.
- Edward, J. T. (1970) *J. Chem. Ed.* **47**, 261–270.
- Richtering, W. H., Burchard, W., Jahns, E. & Finkelmann, H. (1988) *J. Phys. Chem.* **92**, 6032–6040.
- Archer, D. B. (1976) *Biochim. Biophys. Acta* **436**, 68–76.
- Krawczyk, J. & Cukiernan, S. (1991) *Biochim. Biophys. Acta* **1063**, 60–66.
- Puchwein, G., Pfeuffer, T. & Helmreich, E. J. M. (1974) *J. Biol. Chem.* **249**, 3232–3240.

Received March 26, 1993

Accepted September 20, 1993